JOURNAL OF PROPULSION AND POWER
Vol. 24, No. 6, November–December 2008

Study on the Operation of Pulse-Detonation Engine-Driven Ejectors

Aaron J. Glaser,* Nicholas Caldwell,* and Ephraim Gutmark†
University of Cincinnati, Cincinnati, Ohio 45221
John Hoke‡ and Royce Bradley§
Innovative Scientific Solutions, Inc., Dayton, Ohio 45440
and
Frederick Schauer¶
U.S. Air Force Research Laboratory,
Wright–Patterson Air Force Base, Ohio 45433

DOI: 10.2514/1.37869

Experimental studies were performed to improve the understanding of the operation of ejector augmenters driven by a pulse-detonation engine. The research employs an H_2-air pulse-detonation engine at an operating frequency of 30 Hz. Static pressure was measured along the interior surface of the ejector, including the inlet and exhaust sections. Thrust augmentation provided by the ejector was calculated by integration of the static pressure measured along the ejector geometry. The computed thrust augmentation was in good agreement with that obtained from direct thrust measurements. Both straight and diverging ejectors were investigated. The diverging ejector pressure distribution shows that the diverging section acts as a subsonic diffuser and has a tremendous impact on the behavior of the inlet entrainment flow. Static pressure data were also collected for various ejector axial positions. These data supported the thrust augmentation trends found through direct thrust measurements. Specifically, the optimum axial placement was found to be downstream of the pulse-detonation engine near $x/D_{\mathrm{PDE}} = +2$, whereas upstream placements tend to result in decreasing thrust augmentation. To provide a better explanation of the observed performance trends, shadowgraph images of the detonation wave and trailing vortex interacting with the ejector inlet were obtained.

Nomenclature

D_{EJECT}	=	ejector diameter, cm
D_{PDE}	=	detonation tube diameter, cm
DR	=	ejector-to-PDE diameter ratio
ff	=	fill fraction
L_{EJECT}	=	ejector length, cm
L_{EXHST}	=	exhaust-section length, cm
L_{STRT}	=	intermediate straight-section length, cm
T_{PDE}	=	PDE-system thrust with no ejector installed, N
$T_{\mathrm{PDE\ EJECT}}$	=	PDE-system thrust with ejector installed, N
x	=	ejector axial position, cm
α	=	thrust augmentation, %

I. Introduction

ALTHOUGH pulse detonation engine (PDE) technology continues to make progress in gaining acceptance in the aerospace community, many hurdles remain in achieving a practical engine system. One of the key challenges for researchers is to make use of the increased efficiency of energy conversion due to detonative-mode combustion by converting it most effectively into a propulsive thrust force. Many approaches have been undertaken in this effort to harness the transient power created by a train of propagating detonation waves [1]. Much initial work was expended on baseline performance characterization, and as a result a wide array of data has been presented in the literature [2–4]. These data have shown the performance trends in terms of thrust and impulse for both single-cycle and multicycle detonation tube operation. As a result of this work, many analytical models have been produced in an attempt to better predict PDE performance [5–7]. It can generally be shown that the specific impulse generated by a detonation wave depends heavily on the Chapman–Jouguet properties of the reactive mixture. This work has been supported by a large number of computational investigations, ranging from single-cycle predictions to limit-cycle studies [8–11]. Because of the inherent experimental difficulty in capturing unsteady flow phenomena in such a high-pressure, high-temperature environment, these studies have been vital to the understanding of the transient detonation process. This foundation of previous experimental and computational work has suggested that the use of ejector augmenters using a PDE as the primary driver may be an effective way to increase system thrust and specific impulse.

In the simplest terms, an ejector is a coaxial duct placed around the exhaust of an engine that performs as a fluidic pump. By entraining the surrounding ambient air with the primary exhaust flow and directing it into the ejector, the momentum of the engine exhaust flow is increased, leading to the generation of a larger system thrust force [12]. The theory and application of ejectors with regard to a steady primary flow are well established [13,14]. In this type of situation, the secondary flow is entrained primarily through viscous shear mixing [15,16]. Previous research has shown that unsteady ejectors tend to produce more thrust augmentation than steady-flow ejectors [17–19]. According to Wilson et al., the increased performance of unsteady ejectors can be attributed to a more efficient energy-transfer process between the primary and secondary flows that results from the dominant effects of the starting vortex [20]. Because PDEs are

Presented as Paper 0447 at the 45th AIAA Aerospace Sciences Meeting and Exhibit, Reno, NV, 8–11 January 2007; received 3 April 2008; revision received 28 July 2008; accepted for publication 28 July 2008.

*Graduate Research Assistant, Department of Aerospace Engineering, ML0070. Student Member AIAA.
†Professor and Ohio Eminent Scholar, Department of Aerospace Engineering, ML0070. Fellow AIAA.
‡Research Engineer, 2766 Indian Ripple Road. Senior Member AIAA.
§Senior Scientist, 2766 Indian Ripple Road.
¶Mechanical Engineer, AFRL/PRTC, Building 490. Senior Member AIAA.

highly unsteady devices that generate shock waves and strong vortex rings, PDE-driven ejectors have the potential to be highly effective at providing thrust augmentation.

Experimental work has confirmed that PDE-driven ejectors are extremely effective in thrust augmentation. These studies have quantified both the effects of PDE operating parameters and important ejector geometric parameters such as the internal surface geometry. A study by Glaser et al. [21] carried out using several ejector configurations showed maximum thrust augmentation levels of $\alpha = 30\%$ for straight ejectors and $\alpha = 66.5\%$ for an optimized diverging ejector geometry driven by a completely filled detonation tube. Here the thrust augmentation α is defined as the percent increase in thrust compared to the baseline detonation tube without an ejector. Based on a large body of experimental work, it is apparent that diverging ejectors are much more effective at producing thrust augmentation than straight ones. The increased augmentation by diverging ejectors has commonly been attributed to the additional thrust surface area of the diverging section; however, inherent in that explanation is the possibly false assumption that a positive net pressure acts on the diverging section to create a thrust force. It has also been observed that ejector performance is extremely sensitive to the axial position of the ejector inlet relative to the PDE tube exit. In most cases downstream ejector placement provides optimum levels of thrust augmentation [21–24]; however, some researchers have found evidence to the contrary [25,26]. For the straight and diverging ejector configurations previously tested by Glaser et al. [21], the optimum axial position was found to be downstream at $x/D_{\text{PDE}} = +2$.

By measuring the static pressure along the interior surface of various ejector geometries, the current effort seeks to increase the overall understanding of PDE-driven ejector systems. To supplement these data, high-speed shadowgraph flow visualizations were also obtained to provide a better explanation of the observed performance trends. Comparisons were also made between these data and ejector performance data obtained through direct thrust measurements. Results from this study provide insight into the governing flow dynamics and mechanisms responsible for thrust augmentation in PDE-driven ejector systems and better explain the role of the diverging exhaust section in augmenting thrust.

II. Experimental Setup

A. Description of PDE System

Experimental testing for the current study was carried out at the U.S. Air Force Research Laboratory PDE Test Facility at Wright–Patterson Air Force Base [3]. The detonation tube was constructed of type-316 stainless steel, and the geometry tested had an inner diameter of 5.08 cm and a length of 154.94 cm. The system was operated in a premixed manner, using nonpreheated hydrogen and air as the reactants injected at approximately 21°C. Injection of fuel and air into the detonation tube was accomplished using a mechanical valve system that was constructed from a modified four-cylinder automotive valve head with four valves per cylinder driven with a variable-speed electric motor. While the two intake ports were used to deliver premixed hydrogen and air, the two exhaust ports delivered purge air. The purge air cycle was used to cool the detonation tube and provide a buffer between the hot combustion products and the fresh reactants being injected into the tube for the next cycle. Because of the nature of automotive valving, the division of the cycle timing for various events such as fill time, purge time, and detonation time was fixed at one-third of the total cycle. Spark ignition was accomplished using a capacitive-discharge, stock automotive spark system that delivered 105 mJ of energy per pulse. To accelerate the deflagration-to-detonation transition process, a Shchelkin-type spiral with an overall length of 40.64 cm was mounted near the headwall, extending nearly 26% of the detonation tube length.

The PDE system was mounted on a damped thrust stand that was designed to measure the time-averaged thrust generated by the PDE. The thrust stand consisted of linear pillow-block bearings riding along a pair of linear bearing rails. The PDE was allowed to move freely on the rails, but its motion was resisted by springs to prevent resonance effects. To remove the effects of static friction, a novel approach was used by which the PDE was continuously moved forward and backward by a linear pneumatic actuator. Because the actuator produces a net-zero average force, the average position of the thrust stand is a function of the PDE average thrust. The thrust stand was calibrated by placing static weights on a pulley/cable system to simulate a thrust force and measuring the average position of the thrust stand with a displacement sensor. The maximum uncertainty of the thrust stand, which was determined through repeated calibration tests, was found to be ± 1.1 N for the range of PDE thrust loading observed during these tests.

Operation of the PDE system was computer controlled by means of a LabView interface program. This LabView interface provided the flexibility to specify engine operating parameters such as PDE operating frequency, fill fraction, and equivalence ratio. Unless otherwise stated, all of the current tests were performed at an operating frequency of 30 Hz and an equivalence ratio of 1.0. Ionization probes were mounted along the detonation tube length to verify that Chapman–Jouguet (CJ) detonations were obtained. Detonation wave speeds measured throughout experimentation all fell within ± 100 m/s of the theoretical CJ wave speed of 1957 m/s. Data from these sensors were collected at 5 MHz using a 16-channel data acquisition system. This fast sampling rate was adequate for accurate resolution of the detonation wave speed.

B. Ejector Hardware and Instrumentation

To determine the effect of the ejector hardware on the thrust generated by the PDE, the ejectors tested were mounted coaxially to the detonation tube at various positions relative to the PDE exit plane. Two parallel rails were mounted above the PDE which extended beyond the length of the detonation tube. By suspending the ejectors from these rails at different locations, the axial position x of the ejector inlet was able to be varied from -12 to $+6$ tube diameters from the PDE tube exit plane. A negative axial position value corresponds to the ejector inlet placed upstream of the PDE exit, with the ejector overlapping the detonation tube. Similarly, a positive value of axial position corresponds to a situation in which the ejector is mounted downstream of the detonation tube exit.

Two ejector geometries were used during these tests, each consisting of an inlet section, an intermediate straight section, and an exhaust section as shown in Fig. 1b. With the exception of the exhaust section, the two ejectors were identical: one exhaust section was straight whereas the other was diverging. The geometric parameters of the current ejectors were chosen based on results from previous optimization studies [21]. The diameter of the ejector D_{EJECT} was defined as the diameter of the intermediate straight section because this was the minimum diameter for any given ejector geometry. For the current work, D_{EJECT} was held at a fixed value of 13.97 cm. The ejector-to-PDE diameter ratio DR of 2.75 was therefore constant throughout the testing. Based on previous ejector experiments, this value is near the optimum diameter ratio for thrust augmentation [20,22,24]. The inlet used for this testing had a rounded inlet lip with a radius of 3.81 cm. This has been found through previous research to be an important geometric parameter affecting both the internal flowfield and the performance of an ejector [27,28]. The overall nondimensional length of the ejectors was $L_{\text{EJECT}}/D_{\text{EJECT}} = 5.6$, the length of the intermediate straight section was $L_{\text{STRAIGHT}}/D_{\text{EJECT}} = 3$, and the exhaust section had a length of $L_{\text{EXHST}}/D_{\text{EJECT}} = 2.36$. The two exhaust sections tested had half-angle divergences of 0 and 4 deg.

To facilitate the static pressure measurements, each ejector was instrumented with 20 pressure ports along the ejector surface. Each pressure port consisted of a 0.0157-cm-diam thru hole on the ejector surface, which transitioned to a 0.0246-cm-diam tube. Seven of the pressure taps were located on the ejector inlet at the angular locations given in Table 1. As shown in Fig. 2, the remaining 13 pressure taps were distributed along the ejector body: seven were placed on the intermediate straight section and six on the exhaust section. Although this figure depicts an ejector with a straight exhaust section, the diverging exhaust section also had surface pressure taps at the

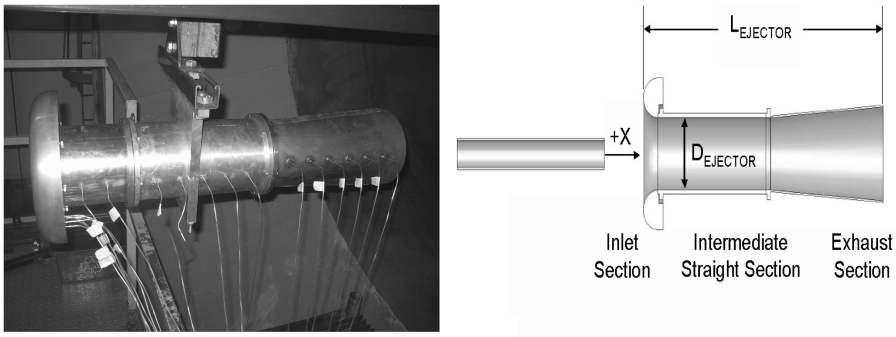

a) b)

Fig. 1 a) Photograph of the installed ejector and b) diagram of ejector geometry used for current work.

same locations. Pressure was measured using a NetScanner Model 9116 Pressure Scanner incorporating 16 silicon piezoresistive pressure sensors, each sampling at a frequency of 1 Hz. Because the pressure measurement system had the ability to sample 16 pressure signals, only 16 of the 20 available ejector pressure taps could be used at a given time. The pressure ports used for the current study are shown schematically in Fig. 2. Each pressure port on the ejector was connected to its corresponding pressure sensor by a 0.0246-cm-diam flexible tube of ∼2.5 m length. Because of the setup of the current system, the dynamic nature of the pressure field was not captured. The length of tubing used between the sensors and the surface pressure taps had the effect of damping out the high-frequency pressure oscillations that are normally associated with PDE operation and had an averaging effect on the pressure history. As a result, the 1-Hz pressure measurement system provided a measure of the time-averaged static pressure at the specified locations. However, high-frequency changes in the pressure field were incapable of being measured and individual detonation events were unable to be discerned in the measurements.

For each data point collected, the PDE was operated for a duration of ∼45 s. To assess the variability of the experimental results, three test runs were performed for each configuration studied. A typical static pressure time history measured on the ejector surface is shown in Fig. 3. Before detonation, cold air is pulsed through the PDE injection valves to allow sufficient time for the desired flow rate to stabilize. This initial unsteady cold flow causes flow entrainment into the ejector and hence a decreased pressure on the ejector inlet, shown by the initial gauge pressure of −1.03 kPa in Fig. 3. After the PDE begins to detonate, the pressure drops to a lower plateau, indicating an increase in flow entrainment. It can be observed that although the measured pressure signal is reasonably steady due to the damping nature of the measurement setup as discussed above, the signal does have a fluctuating component. For all results reported in the current study, the sample mean of the fluctuating pressure was calculated to yield a single value for the static pressure at that sample location. For the case shown, the mean PDE-fired static pressure measured on the ejector inlet at pressure tap 7 was −2.62 kPa. The uncertainty of the static pressure was evaluated statistically by determining the standard deviation of the mean pressure averaged over a representative sample of data sets. By this method, the mean pressure data reported in the current study have an average associated uncertainty of ±0.3 kPa as shown by the error bars in Fig. 3.

Table 1 Locations of pressure taps on ejector inlet section

Tap no.	Tap position, deg
1	0
2	30
3	60
4	90
5	120
6	150
7	165

III. Results and Discussion

A. Straight Ejector Surface Pressure Distribution

The surface pressure distribution measured on a straight ejector is shown in Fig. 4. Results are compared for two primary unsteady driver sources. The first source is a PDE, and the second is an unsteady cold jet, both operating at a frequency of 30 Hz. Both driver sources exhibit similar trends in ejector pressure distribution. For example, it can be observed that the entrained flow being directed into the ejector causes a significant pressure drop on the inlet, thus producing positive thrust on the ejector. The minimum inlet pressure occurred at pressure tap 7, which is at an angle of 165 deg as previously defined. It can also be observed that the outer area of the inlet, pressure taps 1 and 2, did not experience a pressure decrease and thus did not contribute to providing thrust augmentation. This finding implies that the entire rounded portion of the inlet may not be necessary, as comparable performance might be achieved with a simplified inlet design. With a straight ejector, the only surface capable of causing a thrust force is the ejector inlet, and hence a larger negative inlet pressure would always lead to an increase in thrust augmentation. Just downstream of the inlet section, the pressure is observed to rise quickly and a region consistent with separated flow is observed at pressure tap 8. Because the pressure rise is observed to occur in both the PDE and the subsonic cold flow case, it is unlikely that it is due to the presence of a stationary shock wave located in the ejector, but rather flow separation following the flow turning around the ejector inlet. The flow separation is probably due to the strong adverse pressure gradient and large inlet turning angle experienced by the entrainment air. Through the remainder of the straight ejector, static pressure is found to rise gradually until ambient pressure at the ejector exit is reached. The flow area is constant throughout the straight ejector. The rising static pressure is attributed to the primary jet mixing with the slower entrained flow throughout the extent of the ejector. By integrating the measured static pressure over the ejector surface geometry, the amount of thrust augmentation provided by the straight ejector configuration with $ff = 1.0$ was calculated. Defining thrust augmentation as the percent increase in thrust compared to the baseline detonation tube without an ejector,

$$\alpha = \frac{T_{\text{PDE EJECT}} - T_{\text{PDE}}}{T_{\text{PDE}}} \tag{1}$$

the computed augmentation was found to be 26.1%, which is slightly lower than the augmentation of 30.0% obtained by direct thrust measurements [21]. This previous study reported the absolute uncertainty of the thrust stand measured augmentation to be ±2.5%. An uncertainty analysis was performed to determine the uncertainty associated with the pressure derived thrust augmentation of the current study. As previously shown, the pressure measurements have an average uncertainty of ±0.3 kPa. Through a standard propagation of error analysis, it was determined that the reported pressure uncertainty translates into an absolute thrust augmentation uncertainty of ±7.7%.

Figure 5 presents shadowgraph flow visualizations showing the differences between a detonation and cold flow primary driver. The

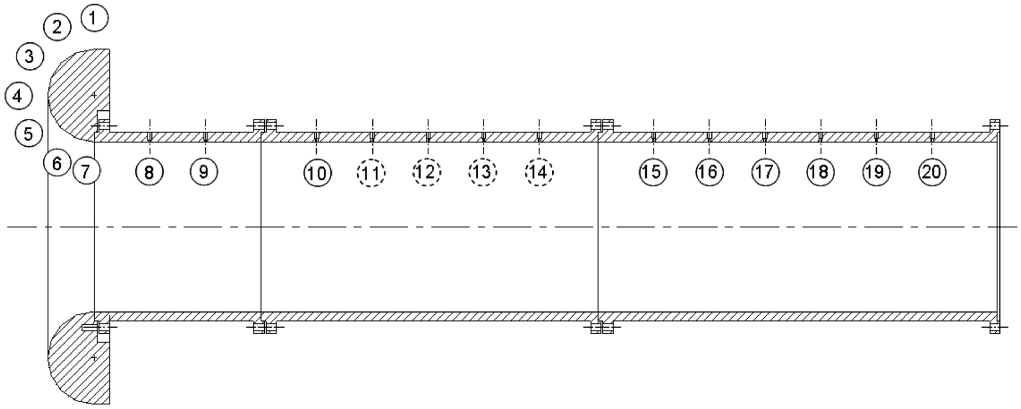

Fig. 2 Placement of pressure sampling ports on ejector interior surface. Solid circles denote ports used during the current study.

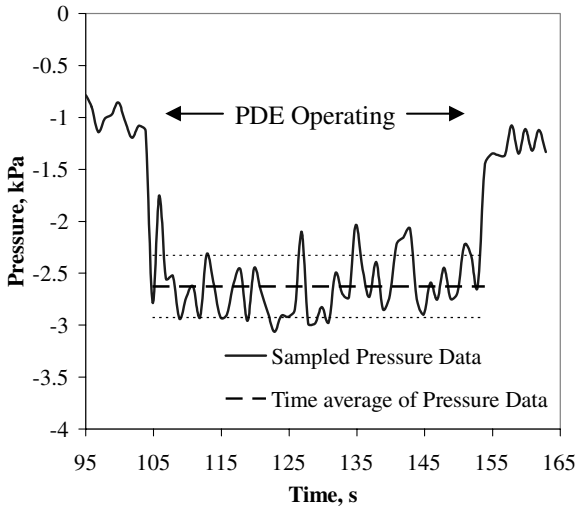

Fig. 3 Pressure history measured at pressure tap 7. The configuration tested was a straight ejector with $x/D_{\mathrm{PDE}} = +2$ and $ff = 1.0$.

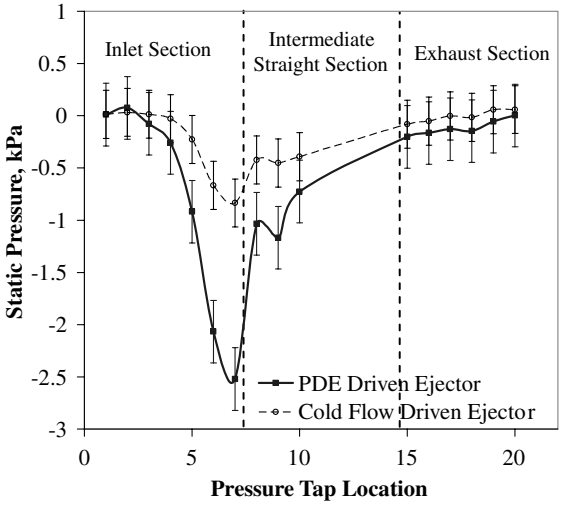

Fig. 4 Ejector surface pressure distribution. The configuration tested was a straight ejector with $x/D_{\mathrm{PDE}} = +2$, and $ff = 1.0$.

visualizations were performed using a 2.54-cm-diam PDE operating at 20 Hz with a straight ejector. In the top row of images, the diffracting detonation wave with trailing vortex structure can be seen. In the bottom row, the vortex structure of the cold flow pulsation can be seen propagating toward the ejector. The time scales are clearly different for the two cases because the velocity of the cold flow starting vortex is much lower than the detonation wave speed. The cold flow vortex is observed to increase in diameter at locations near the tube exit, but then attains a nearly constant diameter as it continues to travel forward. In contrast, the detonation-driven vortex structure exhibits rapid growth until it reaches the ejector inlet. It can also be observed that when the detonation-driven vortex reaches the ejector inlet, its diameter is noticeably larger than that of the cold flow vortex. These results are consistent with experimental unsteady ejector performance measurements which have shown that the optimum ejector-to-driver diameter ratio is larger for PDE-driven ejectors than for cold flow driven systems.

Portions of a complete PDE-driven ejector cycle are shown in Fig. 6. At a time of 111 μs, the shock wave is observed to reflect and travel backward from the ejector inlet. The Mach disk structure present during the blowdown portion of the PDE cycle is visible near the ejector entrance at 148 μs. In the image corresponding to 222 μs, an interaction can be observed between the exhaust plume and the ejector inlet in the form of a vortical structure attached to the inlet lip. The image at 9065 μs was taken much later in the PDE cycle, when the shock and vortex structure are no longer present and the ejector is entraining flow into the inlet. The pattern of the entrained flow at this time during the cycle appears to show a clustering of the flow streamlines near the inner radius of the inlet, indicative of a higher velocity at this location. Furthermore, it appears that no significant amount of entrained flow is passing over the outer radius of the inlet. These observed trends are consistent with the straight ejector pressure distribution discussed above.

B. Diverging Ejector Surface Pressure Distribution

Previous PDE-driven ejector studies have found significant performance enhancement with the use of a diverging exhaust section. In some cases, thrust measurements indicated that the thrust augmentation of the diverging ejector was approximately 2 times that of the straight ejector.

Figure 7 compares the pressure distribution of a straight and a diverging ejector. Again, it must be emphasized that the measurement system employed does not capture the dynamic nature of the pressure field, but simply describes the time-averaged static pressure at each sensor location. It can be seen that the addition of the diverging exhaust section has a significant impact on the ejector inlet flowfield. The diverging ejector shows a vacuum pressure at tap 7 that is doubled in magnitude over that of the straight ejector. This increase in inlet suction represents additional flow entrainment which leads to an increase in thrust augmentation. Also of importance is the fact that the static pressure along the length of the diverging section is negative, rising to ambient conditions at the ejector exit. This suggests that the performance enhancement afforded by diverging ejectors is not due to a positive thrust force acting on the diverging section area. In fact, the diverging section actually creates a slight drag force due to the negative pressure acting on it. The role of the diverging section appears to be that of a subsonic diffuser, decreasing the flow velocity and increasing the static

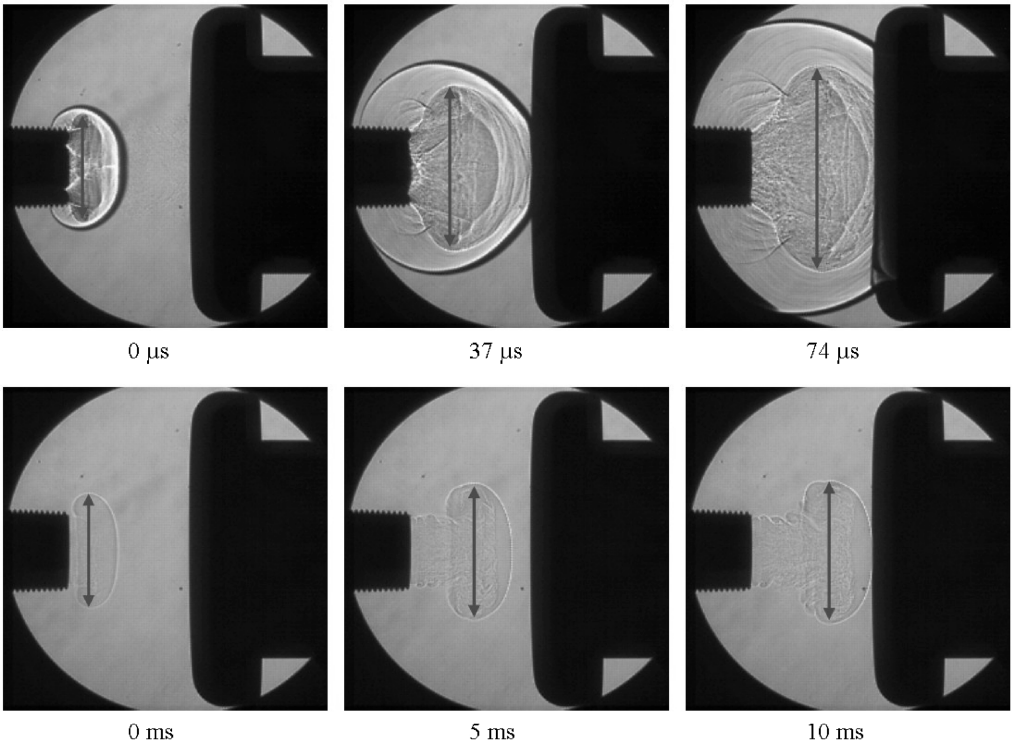

Fig. 5 Shadowgraph images comparing PDE-driven vortex ring (upper images) and cold flow starting vortex (lower images). $ff = 0.6$, $DR = 3$, and $x/D_{\mathrm{PDE}} = +2$.

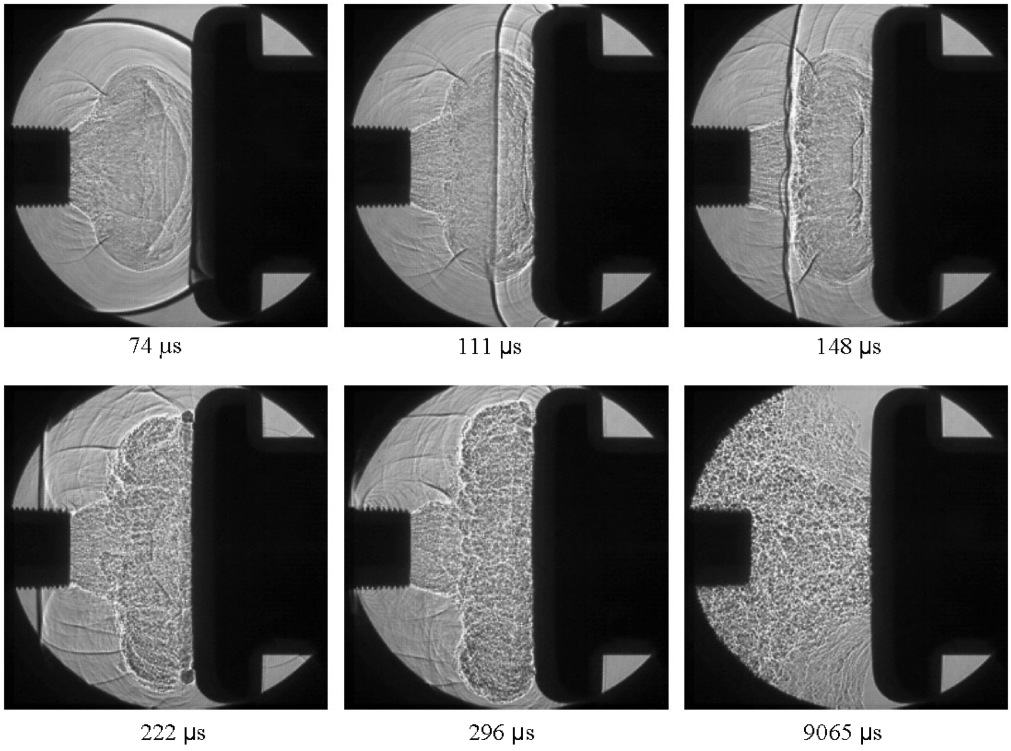

Fig. 6 Sequence of shadowgraph images taken during PDE-driven ejector operating cycle. $ff = 0.6$, $DR = 3$, and $x/D_{\mathrm{PDE}} = +2$.

pressure in the exhaust section. Because the ejector exit-plane boundary condition is that ambient static pressure is achieved in the exhaust jet, the added pressure recovery through the diverging section makes it possible for a decreased inlet pressure to exist while the ejector exit boundary condition is still maintained. In prior experimental testing, the current intermediate straight-section length of $L_{\mathrm{STRAIGHT}}/D_{\mathrm{EJECT}} = 3$ was found to be near the optimum length. Either decreasing or increasing the straight-section length caused a decrease in thrust augmentation. It is speculated that the flow mixing that takes place within the intermediate straight section is beneficial for conditioning the flow before it enters the diffuser. Without a sufficient amount of mixing, the velocity profile entering the diverging section may be prone to separation, causing increased diffuser pressure recovery losses. After the flow is sufficiently mixed, further increase of the straight-section length leads to increased frictional drag forces, and, in turn, decreased thrust augmentation.

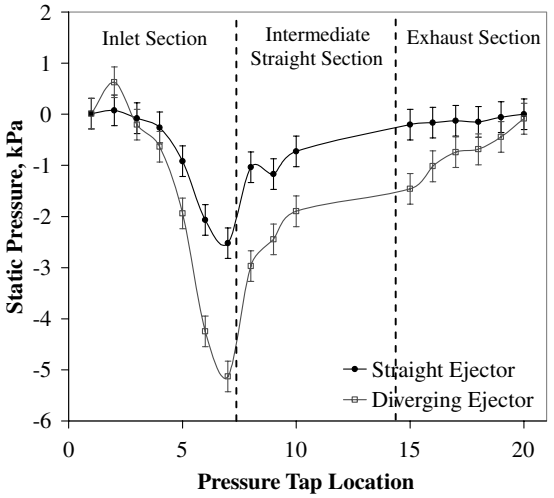

Fig. 7 Static pressure distribution in a straight and diverging ejector. $ff = 1.0$, and $x/D_{\mathrm{PDE}} = +2$.

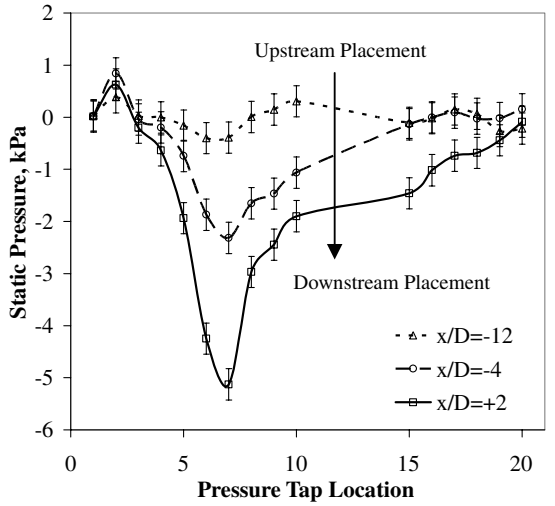

Fig. 9 Effect of axial position on static pressure distribution. Ejector geometry is a diverging ejector with $ff = 1.0$.

Integrating the pressure distribution over the diverging ejector surface geometry yields a calculated thrust augmentation of $\alpha = 50\%$, which is comparable to the thrust augmentation of $\alpha = 66\%$ obtained from direct thrust measurements.

C. Effect of Fill Fraction on Surface Pressure Distribution

Previous studies have shown an inverse relationship between thrust augmentation and the PDE fill fraction at downstream ejector placements [21,23]. For the diverging ejector geometry being considered, thrust augmentation was increased from $\alpha = 66\%$ to $\alpha = 74\%$ by decreasing the fill fraction from $ff = 1.0$ to $ff = 0.6$. Figure 8 shows that decreasing the fill fraction does not significantly alter the pressure distribution over the ejector surface. However, when the fill fraction is decreased, the baseline PDE thrust with no ejector installed decreases at a faster rate than the thrust produced by the ejector. Because thrust augmentation is defined as the change in thrust due to the ejector divided by the baseline PDE thrust, reducing the fill fraction leads to an increased thrust augmentation.

D. Effect of Ejector Axial Position on Surface Pressure Distribution

Ejector performance and internal flowfields have been observed to be sensitive to the axial position of the ejector inlet relative to the PDE tube exit [27]. In most cases, downstream ejector placement provides optimum levels of thrust augmentation [21–24]. For the straight and diverging ejector configurations previously tested by Glaser et al. [21], the optimum axial position was found to be $x/D_{\mathrm{PDE}} = +2$. Figure 9 shows the effect of the axial position on the diverging ejector pressure distribution. It can be seen that as the ejector is moved upstream from $x/D_{\mathrm{PDE}} = +2$, the magnitude of the inlet suction is increased. At the axial location of $x/D_{\mathrm{PDE}} = -12$, it is observed from the pressure distribution that almost no flow is being entrained through the ejector, implying an augmentation near 0%. At this overlap position, a region of slightly positive pressure was also observed in the straight section at pressure tap 10. This overpressure is due to the presence of the detonation tube exit that is located within the ejector.

The axial position trend is more clearly evident in Fig. 10. In this figure static pressure data at tap 7 are plotted for all axial positions tested. The pressure at this location represented the minimum pressure on the inlet for nearly all cases studied and therefore was a good indicator of the amount of flow entrainment into the ejector for a given configuration. The tap 7 pressure data show a minimum pressure near $x/D_{\mathrm{PDE}} = +2$, which is the optimum location for thrust augmentation determined through direct thrust measurements. Placements of the ejector at positions away from the optimum decrease the magnitude of the inlet vacuum pressure, which implies decreasing flow entrainment. Figure 11 shows the thrust augmentation calculated by integration of the ejector pressure distribution compared to that measured through direct thrust measurements. Using both techniques it can be seen that a maximum augmentation is found to occur at $x/D_{\mathrm{PDE}} = +2$, the same position at which the minimum inlet pressure was measured. Although a

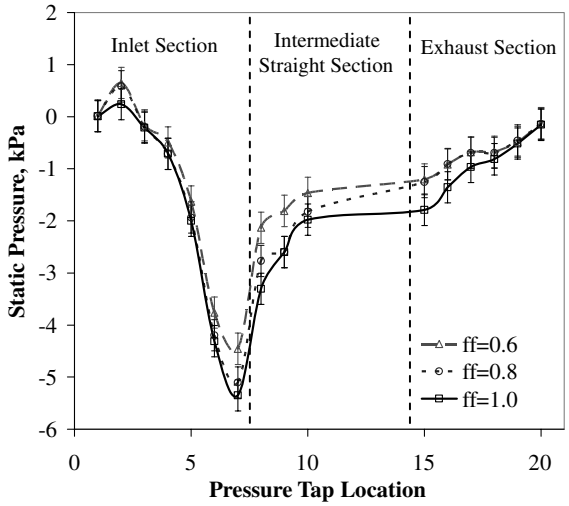

Fig. 8 Effect of the fill fraction on ejector pressure distribution. Ejector geometry is a diverging ejector with $x/D_{\mathrm{PDE}} = +2$.

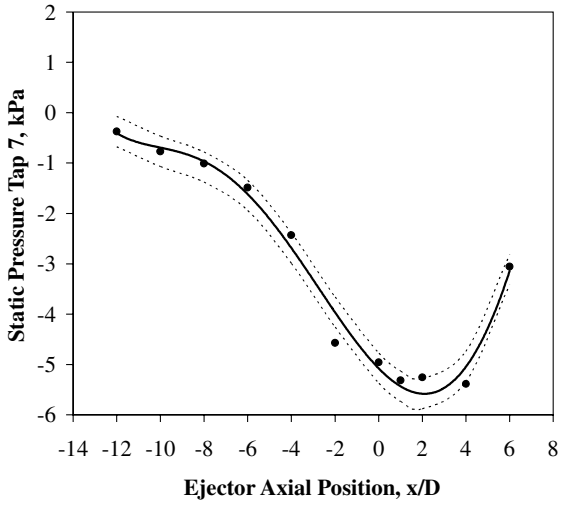

Fig. 10 Effect of axial position on ejector inlet suction.

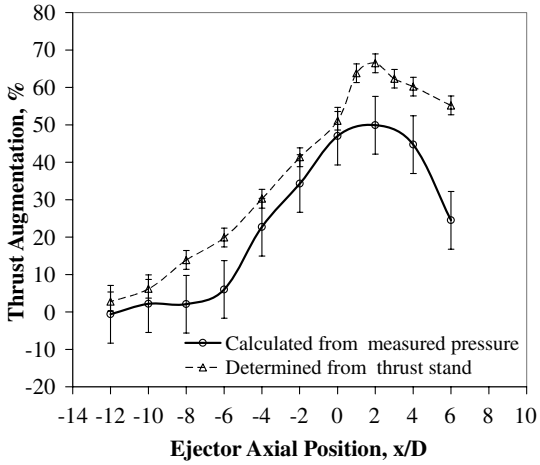

Fig. 11 Effect of ejector position on calculated thrust augmentation. Diverging ejector with $ff = 1.0$.

discrepancy is apparent in the relative magnitudes of thrust augmentation, the overall trend is unmistakable. It is believed that the inability of the integrated pressure distribution to capture the effect that the presence of the ejector has on the detonation tube flowfield is the source of this disparity. The increased blowdown cycle due to the downstream obstruction maintains a higher pressure on the thrust surface of the detonation tube compared to a system with no ejector present. As a result the calculated thrust augmentation based on ejector pressure measurements falls short of the measured thrust augmentation. However, the trend is apparent that placing the ejector upstream of the PDE exit decreases thrust augmentation, while the optimum ejector placement is downstream of the PDE tube exit. Beyond this optimum downstream placement thrust augmentation drops off at a rate similar to the rate of decrease with upstream placement.

IV. Conclusions

An experimental study was performed to investigate the operation of PDE-driven ejectors. To complete this work, both a straight and a diverging ejector were instrumented for static pressure measurements. Analysis of the straight ejector pressure distribution and shadowgraph images showed that a majority of the entrainment flow acceleration near the rounded inlet occurs at the inner inlet radius. This implies that the outer surface of the inlet is not significant in flow entrainment and thus does not need to be as carefully contoured as the inner section of the inlet. In addition it was found that the role of the diverging exhaust section is to act as a subsonic diffuser. The pressure recovery that takes place in this diffuser has a significant impact on the inlet pressure distribution, increasing the magnitude of the inlet vacuum pressure by a factor of 2. Furthermore, the reason for the inverse relationship between fill fraction and thrust augmentation was studied. It was found that the ejector pressure distribution is not very sensitive to the fill fraction. Finally, the axial placement of the ejector inlet relative to the PDE tube exit plane was studied in detail. By varying the axial position from $x/D_{\mathrm{PDE}} = -12$ to $+6$, the axial location of the maximum inlet suction was found to be near $x/D_{\mathrm{PDE}} = +2$. Moving the ejector farther upstream or downstream resulted in the inlet suction decreasing toward zero. Calculating the thrust augmentation based on integration of the pressure distribution showed a maximum at a position of $x/D_{\mathrm{PDE}} = +2$, matching the optimum axial location for thrust augmentation as determined through direct thrust measurements. The observed trends are consistent with the optimum ejector placement being at a downstream location.

Acknowledgments

The authors would like to acknowledge the Propulsion Directorate at the U.S. Air Force Research Laboratory and Innovative Scientific Solutions, Inc., (ISSI) for providing financial support for this work. The technical support of Curtis Rice of ISSI is also greatly appreciated, as is the assistance of Russell Dimicco of the Gas Dynamics and Propulsion Laboratory at the University of Cincinnati.

References

[1] Kailasanath, K., "Review of Propulsion Applications of Detonation Waves," *AIAA Journal*, Vol. 38, No. 9, 2000, pp. 1698–1708. doi:10.2514/2.1156

[2] Ma, F., Choi, J.-Y., and Yang, V., "Propulsive Performance of Airbreathing Pulse Detonation Engines," *Journal of Propulsion and Power*, Vol. 22, No. 6, 2006, pp. 1188–1203. doi:10.2514/1.21755

[3] Schauer, F., Stutrud, J., Bradley, R., Katta, V., and Hoke, J., "Detonation Studies and Performance Results for a Research Pulse Detonation Engine," *Confined Detonation and Pulse Detonation Engines*, edited by G. Roy, S. Frolov, R. Santoro, and S. Tsyganov, Torus Press, Moscow, 2003, pp. 287–302.

[4] Cooper, M., Jackson, S., Austin, J., Wintenberger, E., and Shepherd, J., "Direct Experimental Impulse Measurements for Detonations and Deflagrations," *Journal of Propulsion and Power*, Vol. 18, No. 5, 2002, pp. 1033–1041. doi:10.2514/2.6052

[5] Zitoun, R., and Desbordes, D., "Propulsive Performance of Pulsed Detonations," *Combustion Science and Technology*, Vol. 144, No. 1, 1999, pp. 93–114. doi:10.1080/00102209908924199

[6] Wintenberger, E., Austin, J., Cooper, M., Jackson, S., and Shepherd, J., "Analytical Model for the Impulse of Single-Cycle Pulse Detonation Tube," *Journal of Propulsion and Power*, Vol. 19, No. 1, 2003, pp. 22–38. doi:10.2514/2.6099

[7] Wintenberger, E., and Sheperd, J., "Model for the Performance of Airbreathing Pulse-Detonation Engines," *Journal of Propulsion and Power*, Vol. 22, No. 3, 2006, pp. 593–602. doi:10.2514/1.5792

[8] Ebrahimi, H., and Merkle, C., "Numerical Simulation of a Pulse Detonation Engine with Hydrogen Fuels," *Journal of Propulsion and Power*, Vol. 18, No. 5, 2002, pp. 1042–1048. doi:10.2514/2.6053

[9] Li, C., and Kailasanath, K., "Partial Fuel Filling in Pulse Detonation Engines," *Journal of Propulsion and Power*, Vol. 19, No. 5, 2003, pp. 908–916. doi:10.2514/2.6183

[10] Wu, Y., Ma, F., and Yang, V., "System Performance and Thermodynamic Cycle Analysis of Airbreathing Pulse Detonation Engines," *Journal of Propulsion and Power*, Vol. 19, No. 4, 2003, pp. 556–567. doi:10.2514/2.6166

[11] Tangirala, V., Dean, A., Chapin, D., Pinard, P., and Varatharajan, B., "Pulsed Detonation Engine Processes: Experiments and Simulations," *Combustion Science and Technology*, Vol. 176, No. 10, 2004, pp. 1779–1808. doi:10.1080/00102200490487689

[12] Viets, H., "Thrust Augmenting Ejector Analogy," *Journal of Aircraft*, Vol. 14, No. 4, 1977, pp. 409–411. doi:10.2514/3.44603

[13] Keenan. J. H., Neumann, E. P., and Lustwerk. F., "An Investigation of Ejector Design by Analysis and Experiment," *Journal of Applied Mechanics*, Vol. 17, No. 3, 1950, pp. 299–309.

[14] Quinn. B., "Ejector Performance at High Temperature and Pressures," *Journal of Aircraft*, Vol. 13, No. 12, 1976, pp. 948–954. doi:10.2514/3.44561

[15] Quinn, B., "Compact Ejector Thrust Augmentation," *Journal of Aircraft*, Vol. 10, No. 8, 1973, pp. 481–486. doi:10.2514/3.60251

[16] Arbel, A., Shklyar, A., Hershgal, D., Barak, M., and Sokolov, M., "Ejector Irreversibility Characteristics," *Journal of Fluids Engineering*, Vol. 125, No. 1, 2003, pp. 121–129. doi:10.1115/1.1523067

[17] Kentfield, J., "Fundamentals of Idealized Airbreathing Pulse-Detonation Engines," *Journal of Propulsion and Power*, Vol. 18, No. 1, 2002, pp. 77–83. doi:10.2514/2.5900

[18] Paxson, D., Wernet, M., and Wentworth, J., "Experimental Investigation of Unsteady Thrust Augmentation Using a Speaker-Driven Jet," *AIAA Journal*, Vol. 45, No. 3, 2007, pp. 607–614. doi:10.2514/1.18449

[19] Lockwood, R., "Interim Summary Report on Investigation of the Process of Energy Transfer from an Intermittent Jet to Secondary Fluid in an Ejector-Type Thrust Augmenter," Hiller Aircraft Rept. No. ARD-286, March 1961.

[20] Wilson, J., Sgondea, A., Paxson, D., and Rosenthal, B., "Parametric Investigation of Thrust Augmentation by Ejectors on a Pulse Detonation Tube," *Journal of Propulsion and Power*, Vol. 23, No. 1, 2007, pp. 108–115. doi:10.2514/1.19670

[21] Glaser, A., Caldwell, N., Gutmark, E., Hoke, J., Bradley, R., and Schauer, F., "Performance Measurements of Straight and Diverging Ejectors Integrated with a Pulse Detonation Engine," AIAA Paper 2006-1022, 2006 [*Combustion Science and Technology* (submitted for publication)].

[22] Rasheed, A., Tangirala, V., Pinard, P., and Dean, A., "Experimental and Numerical Investigations of Ejectors for PDE Applications," AIAA Paper 2003-4971, 2003.

[23] Allgood, D., and Gutmark, E., "Performance Measurements of Pulse Detonation Engine Ejectors," AIAA Paper 2005-0223, 2005.

[24] Glaser, A., Caldwell, N., Gutmark, E., Hoke, J., Bradley, R., and Schauer, F., "Effects of Tube and Ejector Geometry on the Performance of Pulse Detonation Engine Driven Ejectors," AIAA Paper 2006-4790, 2006.

[25] Canteins, G., Franzetti, F., Zoclonska, E., Khasainov, B., Zitoun, R., and Desbordes, D., "Experimental and Numerical Investigations on PDE Performance Augmentation by Means of an Ejector," *Shock Waves*, Vol. 15, No. 2, 2006, pp. 103–112. doi:10.1007/s00193-006-0006-5

[26] Shehadeh, R., Saretto, S., Lee, S., Pal, S., and Santoro, R., "Experimental Study of a Pulse Detonation Engine Driven Ejector," AIAA Paper 2003-4972, 2003.

[27] Allgood, D., Gutmark, E., Rasheed, A., and Dean, A., "Experimental Investigation of a Pulse Detonation Engine with a Two-Dimensional Ejector," *AIAA Journal*, Vol. 43, No. 2, 2005, pp. 390–398. doi:10.2514/1.8125

[28] Wilson, J., "Effect of Pulse Length and Ejector Radius on Unsteady Ejector Performance," *Journal of Propulsion and Power*, Vol. 23, No. 2, 2007, pp. 345–352. doi:10.2514/1.19665

J. Powers
Associate Editor